Natural diversity uncovers HvP5cs1 regulation and its role in drought stress adaptation and yield sustainability in barley

Asis Shrestha[1], Alexander Fendel[1], Thuy Huu Nguyen[1], Anteneh Adebabay[1], Annika Stina Kullik[1], Jan Benndorf[1], Jens Léon[1], and Ali Naz[1]

[1]Rheinische Friedrich-Wilhelms-Universitat Bonn Institut fur Nutzpflanzenwissenschaften und Ressourcenschutz

May 21, 2022

Abstract

Breeding drought stress tolerance is an integral part of our current and future goals of sustainable agricultural production. In the present study, we examined the natural variation of *HvP5cs1* and demonstrated the utility of a wild barley allele for drought stress adaptation in cultivated barley. Sequencing the 5-end regulatory region among 49 barley accessions identified a genetically distinct allele of *HvP5cs1* promoter from a wild barley ISR42-8. Allele mining of *HvP5cs1* indicated quantitative variation in proline accumulation which was associated with promoter polymorphisms across the cluster of abscisic acid-responsive elements (ABRE), ABRE-related coupling elements, and MYB binding motifs. A near-isogenic line (NIL-143) harboring the *HvP5cs1* allele from the highest proline accumulating wild barley ISR42-8 was developed in cultivated barley Scarlett through marker-assisted backcrossing (BC6). NIL-143 preserved the genetic competence of ISR42-8 to accumulate proline in higher concentrations under drought conditions at seedling and reproductive stages. Under drought stress, NIL-143 maintained superior membrane integrity, reduced pigment damage, and sustained photosynthetic health compared to Scarlett. NIL-143 presented a remarkable improvement in drought stress recovery than Scarlett. Further, the introgression line exhibited improved yield attributes, especially superior grain weight compared to Scarlett under field drought conditions. In conclusion, the present data uncover the genetic regulation of *HvP5cs1* mediated proline accumulation and elucidate its role in drought stress adaptation and yield stability in barley.

Hosted file

`Manuscript.HvP5cs1.allele.docx` available at https://authorea.com/users/484060/articles/569951-natural-diversity-uncovers-hvp5cs1-regulation-and-its-role-in-drought-stress-adaptation-and-yield-sustainability-in-barley

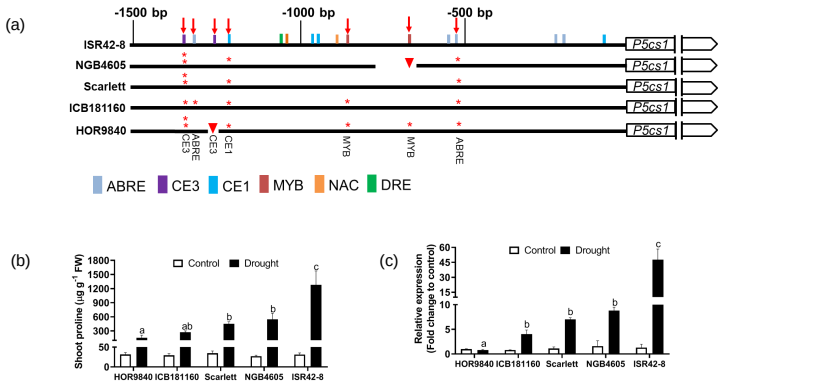

Figure 1: Predicted drought stress-related transcription factor target sequence on *HvP5cs1* promoter. (a) The relative position of *cis*-acting elements detected in *HvP5cs1* promoter. Asterisks indicate the number of SNPs detected across the *cis*-elements. Triangle indicates the site of deletions. (b) Shoot proline concentration in five barley genotypes grown inside an automated climate chamber. Bars represent mean + SE (n = 8). (c) Relative mRNA expression of *HvP5cs1* gene. Bars represent mean + SE (n = 3). Indexed letters above the bars indicate significant differences between the genotypes ($P \leq 0.05$), not sharing the same letter under drought conditions. FW, fresh weight

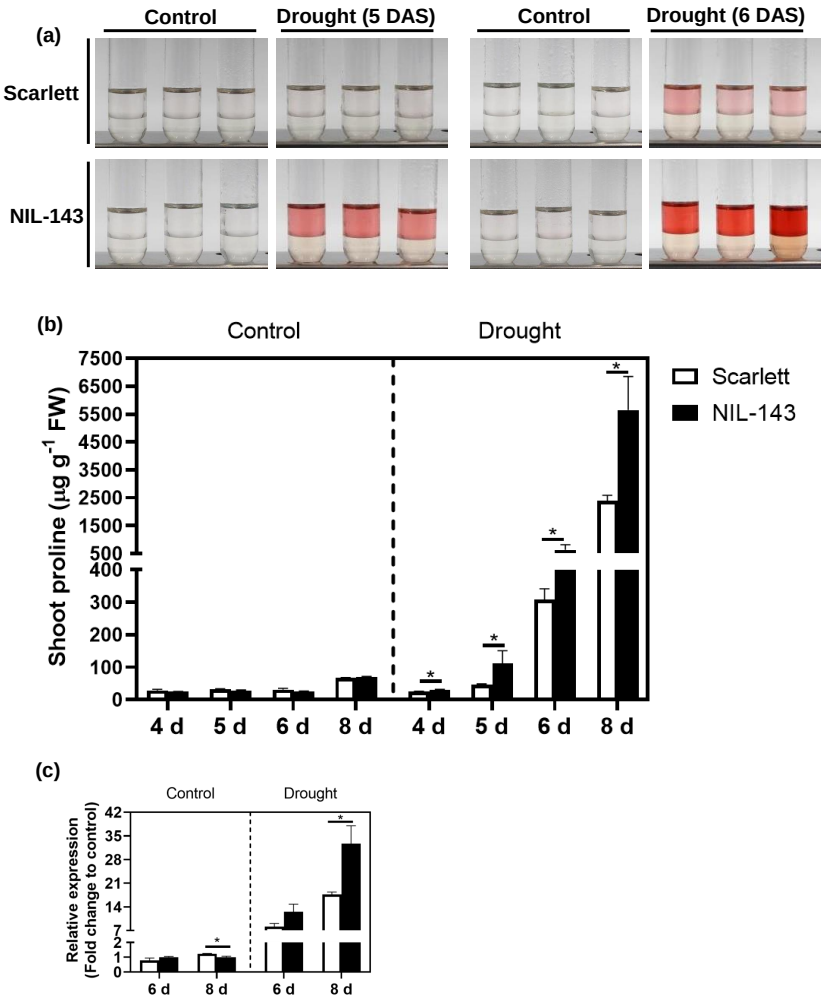

Figure 2: Proline accumulation in Scarlett and NIL-143 at the seedling stage in response to drought stress grown inside an automated climate chamber. Drought treatment was applied to two-week-old seedlings by terminating the water supply. Sampling was done at 4 d, 5 d, 6 d, and 8 d after drought stress before proline measurement. The experiment was performed inside a controlled climate chamber. (a) Chromatophore indicates a free proline reaction product with ninhydrin. Darker color indicates a higher concentration of proline. (b) Shoot proline concentration under control and drought conditions. The graph represents the mean + SE (n = 5). (c) Relative mRNA expression of *HvP5cs1* gene. The graph represents the mean + SE (n = 3). Asterisks indicate significant differences between genotypes (*$P \leq 0.05$) using a student's *t*-test. FW, fresh weight

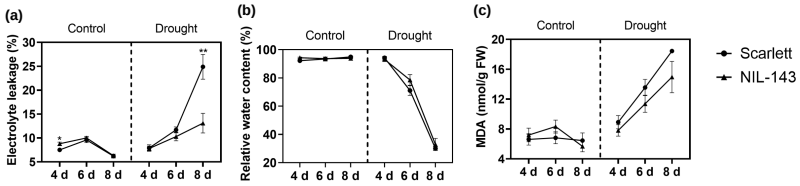

Figure 3. Physiological responses of Scarlett and NIL-143 to drought stress at the seedling stage grown inside an automated climate chamber. The experiment was performed inside a controlled climate chamber. Effect of drought on (a) Electrolyte leakage, (b) Relative water content, and (c) Malondialdehyde (MDA) concentration. Drought treatment was applied to two-week-old seedlings by terminating the water supply. Sampling was done at 4, 6 and 8 d after drought stress to analyze the biochemical and physiological response of plants to drought stress. Bar indicates mean ± SE (n = 5). Asterisks indicate significant differences between genotypes (*$P \leq 0.05$, **$P \leq 0.01$) using student's *t*-test. FW, fresh weight

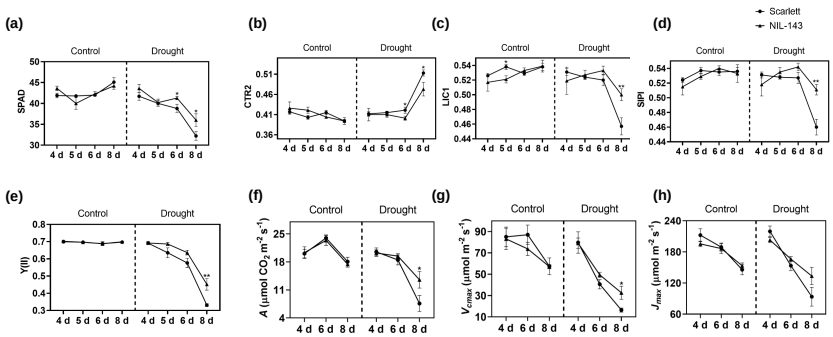

Figure 4. Vegetation indices and photosynthetic traits in Scarlett and NIL-143 under drought stress at the seedling stage grown inside an automated climate chamber. Effect of water stress on (a) soil plant analysis development (SPAD) chlorophyll meter value, (b) Lichtenthaler index 1 (Lic1), (c) structure intensive pigment index (SIPI), (d) Carter index 2 (Ctr2), (e) effective quantum yield of photosystem II (Y(II), (f) rate of CO2 assimilation (*A*), (g) maximum carboxylation rate of rubisco (V_{cmax}), and (h) maximum rate of electron transport (J_{max}). Drought treatment was applied to two-week-old seedlings by terminating the water supply. Photosynthesis-related traits were evaluated at 4, 5, 6 and 8 d after drought stress using MiniPam and gas exchange analyzer by LI-COR. The graph indicates mean ± SE (n = 5). Asterisks indicate significant differences between genotypes (*$P \leq 0.05$, **$P \leq 0.01$) using student's *t*-test.

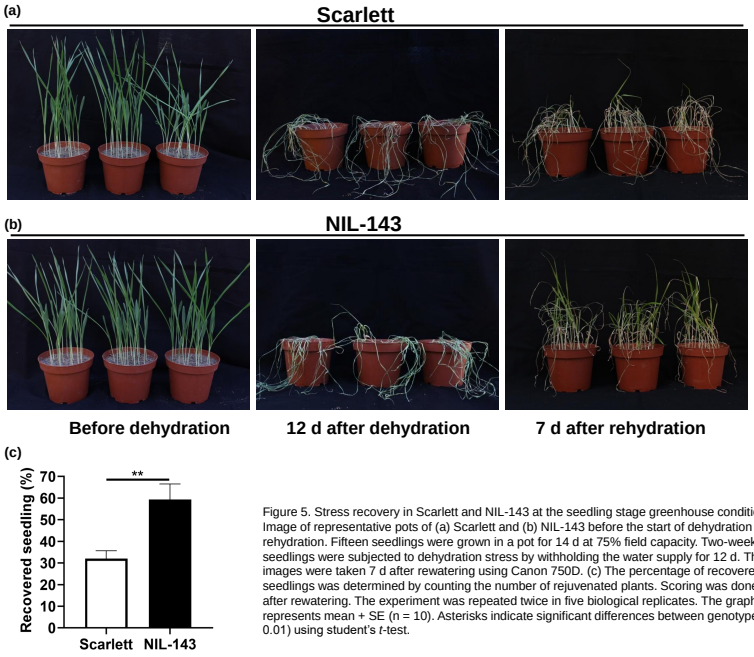

Figure 5. Stress recovery in Scarlett and NIL-143 at the seedling stage greenhouse conditions. Image of representative pots of (a) Scarlett and (b) NIL-143 before the start of dehydration and after rehydration. Fifteen seedlings were grown in a pot for 14 d at 75% field capacity. Two-week-old seedlings were subjected to dehydration stress by withholding the water supply for 12 d. The images were taken 7 d after rewatering using Canon 750D. (c) The percentage of recovered seedlings was determined by counting the number of rejuvenated plants. Scoring was done 14 d after rewatering. The experiment was repeated twice in five biological replicates. The graph represents mean + SE (n = 10). Asterisks indicate significant differences between genotypes (**$P \leq 0.01$) using student's *t*-test.

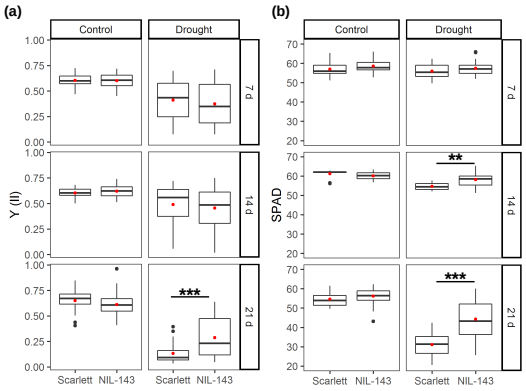

Figure 6. Vegetation index and photosynthetic parameters of Scarlett and NIL-143 in field conditions. Effect of drought stress on (a) effective quantum yield of photosystem II (Y(II)) (b) soil plant analysis development (SPAD) chlorophyll meter value. Scarlett and NIL-143 were grown in 40 cm rows inside a rainout shelter. One plot was regularly irrigated, while drought stress was applied to another plot for 21 d at the heading stage (BBCH 41). Vegetation indexes and photosynthetic traits were scored at 7, 14, and 21 d after stress. The red dot indicates the mean of the distribution. Asterisks indicate significant differences between genotypes (*$P \leq 0.05$, **$P \leq 0.01$, ***$P \leq 0.001$) using student's *t*-test (n = 19 to 45).

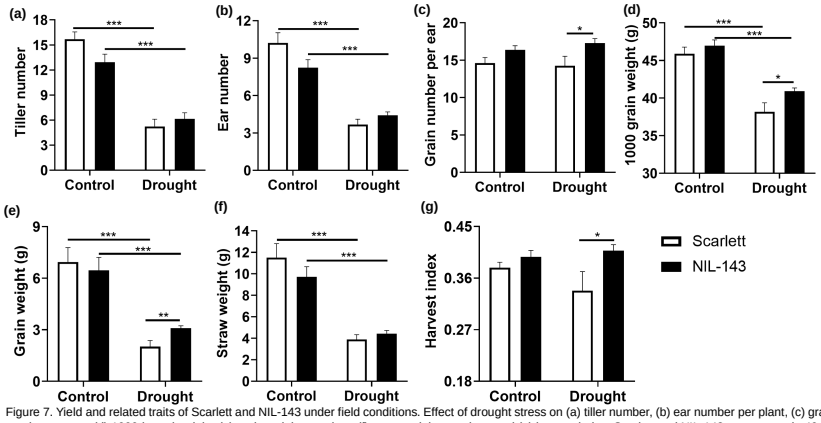

Figure 7. Yield and related traits of Scarlett and NIL-143 under field conditions. Effect of drought stress on (a) tiller number, (b) ear number per plant, (c) grain number per ear, (d) 1000-kernel weight, (e) grain weight per plant, (f) straw weight per plant, and (g) harvest index. Scarlett and NIL-143 were grown in 40 cm rows inside a rainout shelter. One plot was regularly irrigated, while drought stress was applied to another plot for 21 d before the heading stage (BBCH 41). Matured panicles and straw were harvested and oven-dried at 35°C for 72 h. The experiment was performed at Campus Kleinaltendorf, Rheinbach, Germany. The graph represents the mean + SE (n = 10). Asterisks indicate significant differences between genotypes (*$P \leq 0.05$, **$P \leq 0.01$, ***$P \leq 0.001$) using a student's *t*-test.